Planar Near-Field RFID Reader Antenna for Item-Level Tagging

Chihyun Cho, Chuyong Lee, Jeongki Ryoo, and Hosung Choo, *Senior Member, IEEE*

***Abstract*—In this letter, we propose a novel UHF planar near-field antenna for the application of RFID item-level tagging. The proposed antenna was designed to have a strong and uniform H_z-field over a broad antenna aperture to identify the various items with stable reading performance. To obtain a strong near H_z-field, two coupled patches are employed along with a microstrip-line feed, resulting in average H_z of -15 dBA/m on antenna aperture ($30 \times 30 \times 10$ cm^3). We also measured the reading range, and it confirmed that the proposed antenna is suitable for a commercial RFID smart-shelf application.**

***Index Terms*—Item-level tagging (ILT), near field, radio frequency identification (RFID), reader antenna, ultrahigh frequency (UHF) band.**

I. Introduction

RADIO frequency identification (RFID) systems for near-field communications in the ultrahigh frequency (UHF) band have gained much attention since they exhibit a better read rate on lossy dielectric materials, such as garments, drugs, and retail goods [1]–[11]. These RFID systems for near-field communications need a special reader antenna that can produce a strong magnetic field near the antenna aperture in broad regions. For example, a reader antenna that can produce a strong H_z-field of greater than -20 dBA/m (notation of z means that it is perpendicular to the aperture of the reader antenna) is required to detect a small loop tag of 1-cm radius [12]. In addition, the reader antenna should have a thin profile for some applications such as a shelf.

In the UHF band, the loop or solenoid structure, which is widely used in the low-frequency band, is not appropriate to produce strong near magnetic field in the broad region since the generated field from those structures covers only confined regions due to the physically reduced apertures. In our previous work, we proposed the concept of oppositely directed currents (ODCs) to solve this problem, as shown in Fig. 1. The ODCs consist of two currents with a phase difference of about 180°, and H_z is produced strongly between them. Also, the H_z-field can be easily concentrated in a certain target area by appropriately choosing the distance d and strength of amplitude I_1 and I_2 of each current [12].

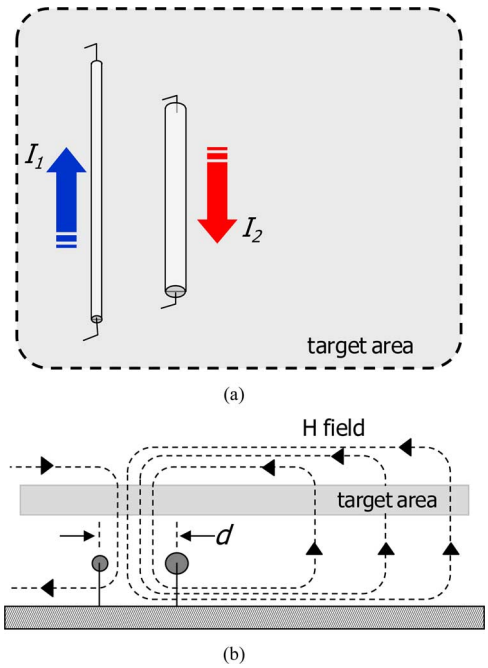

Fig. 1. Concept of ODCs. (a) Top view. Two currents flow oppositely along two wires. (b) Side view. Near magnetic field produced by ODCs is exhibited as arrow lines.

In this letter, we realize the concept of ODCs using two coupled patches with a microstrip line feed to make it suitable for thin-profile shelf applications. The proposed antenna design exhibits an H_z-field of greater than -20 dBA/m over an antenna aperture of about 30×30 cm^2 with a thin profile (less than 2.5 cm). The detailed design parameters are optimized using Pareto genetic algorithm (PGA) in conjunction with FEKO electromagnetic (EM) simulator [13], [14]. We also confirm that the read range is not drastically changed on various target materials.

II. Antenna Structure and Optimization

Fig. 2 shows the proposed RFID reader antenna structure for the shelf. To realize the concept of ODCs, two coupled patches ($L_1 \times W_1, L_2 \times W_2$) are printed on an FR-4 substrate ($\varepsilon_r = 4.2, \tan\delta = 0.02$, thickness $= 1.6$ mm). The uniform distribution of the H_z-field can be achieved with proper current distributions on both the coupled patches by detuning the width, length, and distance between patches. To induce currents on each patch, a microstrip line of $L_3 \times W_3$, fed from the side

Manuscript received May 16, 2011; revised August 14, 2011; accepted September 07, 2011. Date of publication September 29, 2011; date of current version October 17, 2011. This work was supported by the National Research Foundation of Korea under Grant NRF-2010-013-D00055 funded by the Korean Government.

C. Cho is with the Communication R&D Center, Samsung Thales, Seongnam 463-870, Korea.

Chuyong Lee is with ezVille, Inc., Seoul 153-792, Korea.

Jeongki Ryoo is with the Central R&D Center, LS Industrial Systems, Anyang 431-831, Korea.

Hosung Choo is with the School of Electronic and Electrical Engineering, Hongik University, Seoul 121-791, Korea (e-mail: hschoo@hongik.ac.kr).

Color versions of one or more of the figures in this letter are available online at http://ieeexplore.ieee.org.

Digital Object Identifier 10.1109/LAWP.2011.2169929

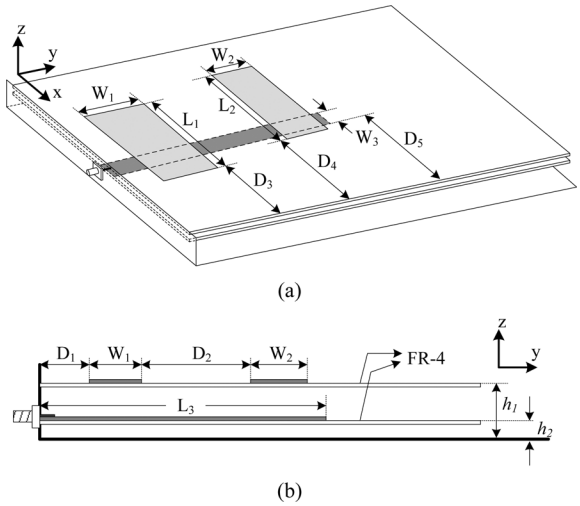

Fig. 2. Proposed planar near field reader antenna using concept of ODCs. (a) Perspective view. (b) Side view.

wall, is inserted between the two patches and the ground plate, and it is also printed on the FR-4 substrate. The amount of induced currents on each coupled patch is dominantly determined by the gap between two substrates of $h_1 - h_2$ and the distance between the side wall and patch of D_1. The detailed design parameters such as $h_1, h_2, W_1, W_2, W_3, L_1, L_2, L_3, D_1, D_2, D_3, D_4$, and D_5 are optimized by PGA, and the antenna performance is predicted using FEKO EM simulator. In the PGA process, the optimized antenna is evaluated by following two cost functions:

$$\text{Cost1} = 1 - \int_s \mathbf{H}_z ds$$
$$\text{Cost2} = 1 - [\max(|\mathbf{H}_z|) - \min(|\mathbf{H}_z|)].$$

Lowering the cost means improving the antenna performances. *Cost1* addresses the strength of the $\boldsymbol{H}_z$-field on the targeted surface area of 30×30 cm^2, and *Cost2* implies the uniformity of the $\boldsymbol{H}_z$-field on the targeted area. The optimized design parameters obtained from the aforementioned optimization process are as follows: $L_1 = 12.51$ cm, $L_2 = 12.12$ cm, $L_3 = 16.87$ cm, $W_1 = 4.58$ cm, $W_2 = 3.44$ cm, $W_3 = 1.91$ cm, $h_1 = 2.2$ cm, $h_2 = 0.54$ cm, $D_1 = 2.11$ cm, $D_2 = 6.4$ cm, $D_3 = 9.52$ cm, $D_4 = 12.08$ cm, $D_5 = 12.92$ cm.

III. Antenna Characteristics

To confirm the optimized result, we measure the antenna performances such as bandwidth, radiation pattern, and near-field distribution. The measured bandwidth ($S_{11} < -10$ dB) is 30 MHz, from 910 to 940 MHz, which entirely covers the required frequency band in Korea (917–923.5 MHz), and it matches well with the simulation result as shown in Fig. 3(a). The operating frequency and input impedance is mainly affected by length of the microstrip line L_3. If L_3 increases, then the resonant frequency of the antenna is shifted to lower band, with slight changes of other performances. Thus, the antenna can be tuned for other operating frequency bands, such as Europe (865–868 MHz) and Japan (952–955 MHz). Although this device is designed for near-field applications, the

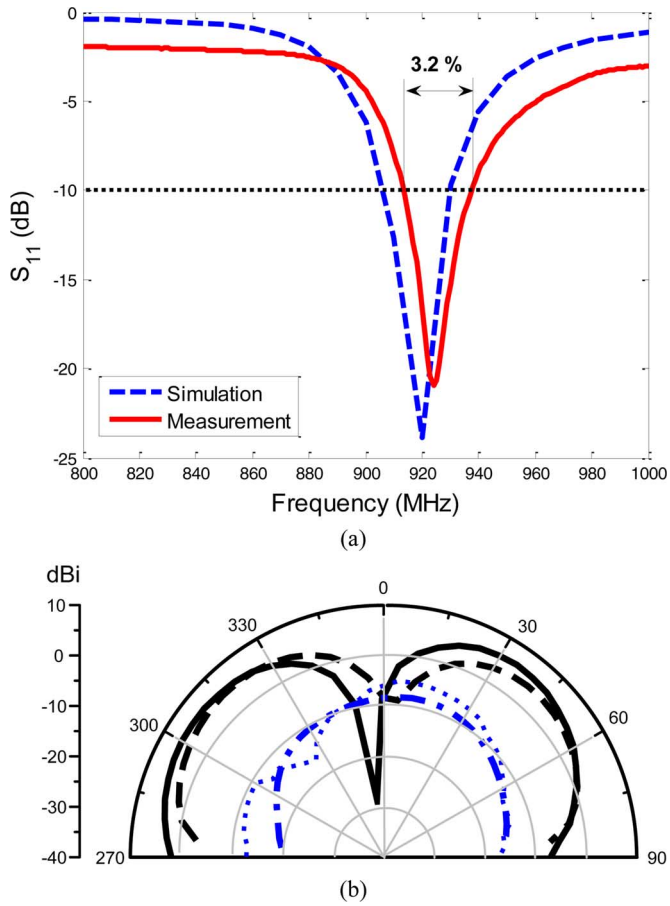

Fig. 3. (a) Simulated (dashed line) and measured (solid line) reflection coefficient. (b) Simulated (dashed line) and measured (solid line) radiation pattern in phi $= 0°$, and simulated (dotted line) and measured (dashed-dotted line) radiation pattern in phi $= 90°$, respectively.

device introduces a certain amount of far-field radiation. Thus, radiation gain patterns are measured to examine the satisfaction of the EIRP regulation. The measured and simulated results are compared in Fig. 3(b), and they agree well with each other. The maximum gain is about 6.8 dBi. Thus, the input power should be lower than 0.832 W (less than 4 W EIRP in Korea). However, the reading performances such as the reading range and reading success tests are conducted with the 1-W input power.

Next, the $\boldsymbol{H}_z$-field is measured using a small loop probe over the surface that is 3 cm above the antenna aperture, as shown in Fig. 4(a). The measured $\boldsymbol{H}_z$ is greater than the specification of -20 dBA/m in most of the target surface region. As we expected, strong and uniform near $\boldsymbol{H}_z$-field is observed along the target surface region. We also examine current distribution by EM simulator, and the result shows that the lengths of induced currents on each patch are about half-wavelength and that they flow in the opposite directions, as shown in Fig. 4(b). As the distance D_2 between two patches increases, the phase difference between two currents also increases, and thus, D_2 should be chosen properly to make currents on two patches with out of phase. Also, the place where the strong $\boldsymbol{H}_z$-field is generated is easily moved when the length and width of each patch is changed. For example, if we reduce the length L_1 or increase

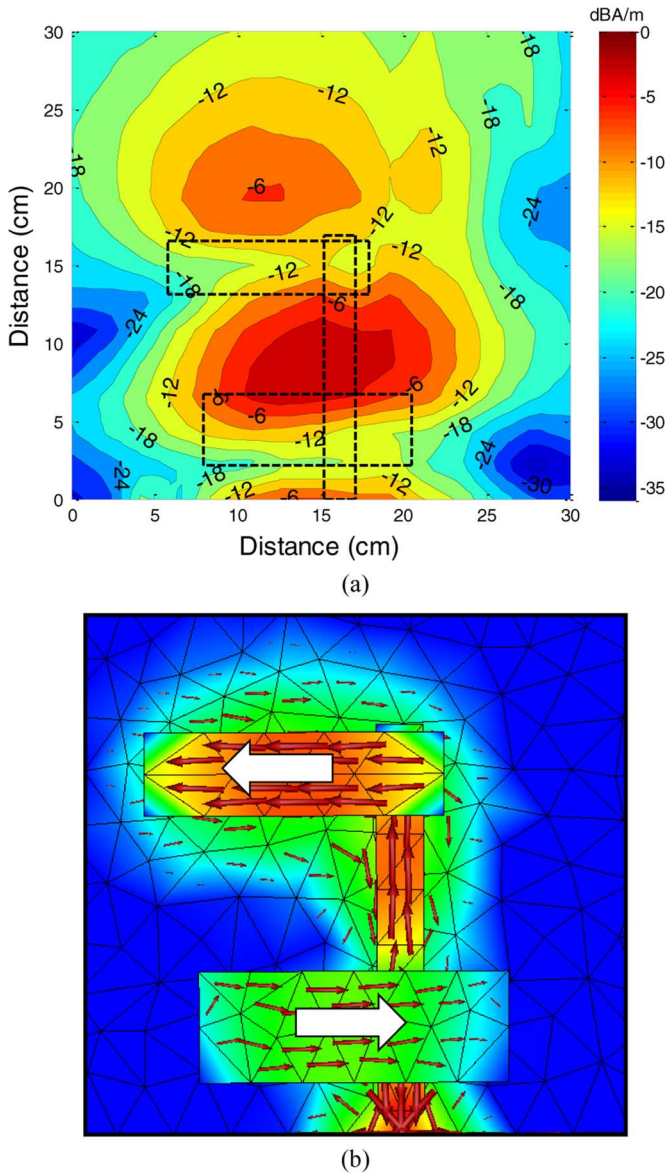

Fig. 4. (a) Measured near $\boldsymbol{H}_z$-field on a surface 3 cm above the antenna aperture. (b) Simulated current distribution using commercial EM simulator.

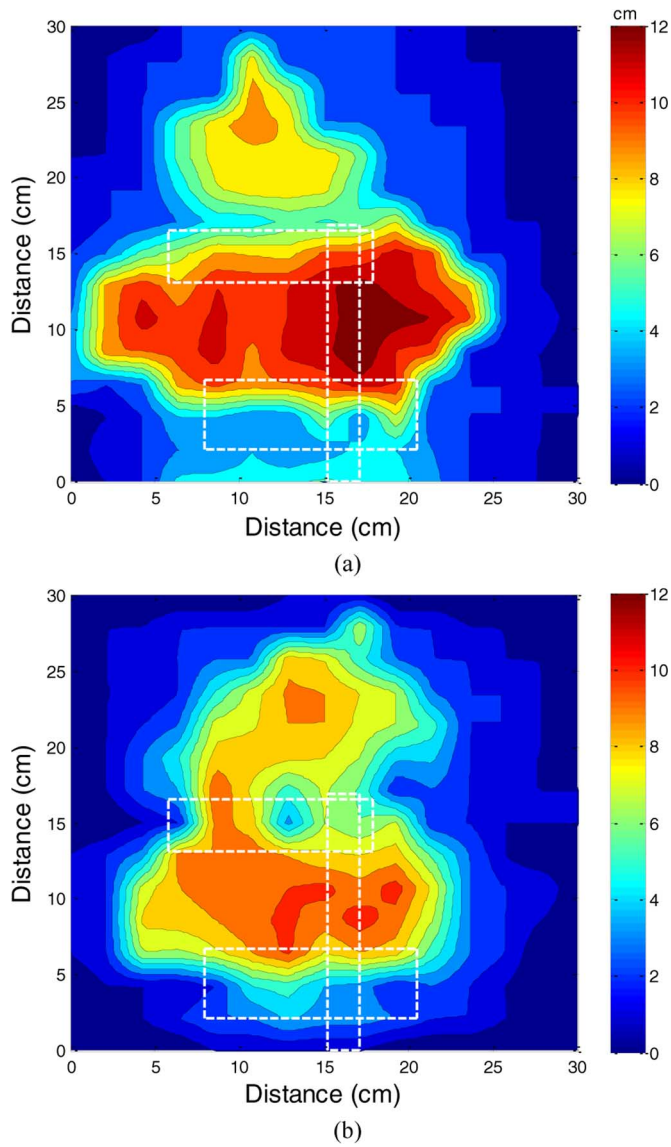

Fig. 5. Measured reading range. (a) Commercial small loop tag is in free space. (b) Commercial small loop tag is attached to the bottom of reagent bottles.

the length L_2 for raising the induced current of the lower patch, then the strong H_z-field is shifted to the feeder.

IV. Reading Performances

Finally, the reading performances of the proposed antenna are measured using a commercial loop tag (1.1×1.1 cm^2) and an RFID reader system [15], [16]. The reading range is measured when the tag is in free space and is attached to the bottom of the reagent bottles, as shown in Fig. 5(a) and (b), respectively. The maximum reading range of 12 and 10 cm is observed for free space and with the reagent bottle. A small variation of the reading range is observed, and this verifies that the adjacent dielectric materials do not significantly affect the reading performance of the proposed antenna.

Next, we measure the total number of readable tag when 100 reagent bottles are placed on top of the antenna aperture. The bottles are empty and they occupy the area of 22×22 cm^2. We also tested the performance by placing various dielectric materials such as wood, water, and foam between the aperture and reagent bottles. Fig. 6(a) shows the measurement setup, and Fig. 6(b) exhibits the resulting success rate with various thicknesses and different dielectric materials. As expected, the total number of readable tag decreases as the thickness of materials increases. A success rate of over 80% is observed for dielectric materials less than 2 cm thick, using three different kinds of materials, and this confirms that the reading performance of the proposed antenna is not significantly affected by the high-dielectric materials.

V. Conclusion

In this letter, we proposed a novel RFID reader antenna for thin-profile shelf. To produce the strong $\boldsymbol{H}_z$-field over the broad surface of the shelf, the concept of opposite directed currents was employed for the proposed design structure. Also, the coupled microstrip-line feeding system was applied to

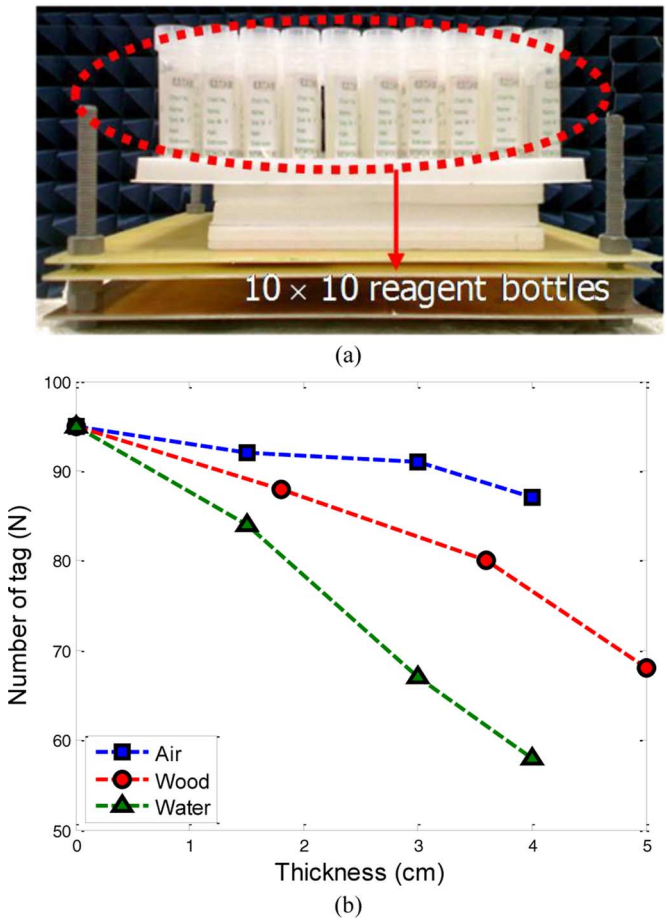

Fig. 6. (a) Measurement setup. (b) Measured total number of readable tag on the various materials.

reduce the antenna profile. The detailed design parameters were optimized to produce the strong $\boldsymbol{H}_z$-field in the target surface area of 30×30 cm^2 using PGA in conjunction with full EM simulator. The optimized antenna showed an average $\boldsymbol{H}_z$-field of -15 dBA/m over the antenna aperture and achieved stable reading performance. The measured results showed that the proposed antenna is applicable for a thin profile near-field reader antenna.

REFERENCES

[1] S. R. Aroor and D. D. Deavours, "Evaluation of the state of passive UHF RFID: An experimental approach," *IEEE Syst. J.*, vol. 2, no. 2, pp. 168–176, Dec. 2007.
[2] A. Shameli, A. Safarian, A. Rofougaran, M. Rofougaran, J. Castaneda, and F. D. De Flaviis, "A UHF near field RFID system with fully integrated transponder," *IEEE Trans. Microw. Theory Tech.*, vol. 56, no. 5, pp. 1267–1277, May 2008.
[3] J. Hong, J. Choo, J. Ryoo, and C. Choi, "A shelf antenna using near-field without dead zones in UHF RFID," in *Proc. IEEE ICIT*, Gippsland, Australia, 2009, pp. 1–4.
[4] C. Lee, C. Cho, J. Ryoo, I. Park, and H. Choo, "Planar near-field RFID reader antenna using opposite-directed currents," in *Proc. IEEE iWAT*, Santa Monica, CA, 2009, pp. 1–4.
[5] X. Qing, C. K. Goh, and Z. N. Chen, "Segmented loop antenna for UHF near-field RFID applications," *Electron. Lett.*, vol. 45, no. 17, pp. 872–873, Aug. 2009.
[6] X. Qing, C. K. Goh, and Z. N. Chen, "UHF near-field RFID reader antenna," in *Proc. Asia–Pacific Microw. Conf.*, Singapore, 2009, pp. 2383–2386.
[7] H.-W. Liu, K.-H. Wu, and C.-F. Yang, "UHF reader loop antenna for near-field RFID applications," *Electron. Lett.*, vol. 46, no. 1, pp. 10–11, Jan. 2010.
[8] Y. S. Ong, X. Qing, C. K. Goh, and Z. H. Chen, "A segmented loop antenna for UHF near-field RFID," in *Proc. IEEE AP-S Int. Symp.*, Jul. 2010, pp. 1–4.
[9] X. Qing, Z. N. Chen, and C. K. Goh, "UHF near-field RFID reader antenna with capacitive couplers," *Electron. Lett.*, vol. 46, no. 24, pp. 1591–1592, Dec. 2010.
[10] X. Qing, C. K. Goh, and Z. N. Chen, "A broadband UHF near-field RFID antenna," *IEEE Trans. Antennas Propag.*, vol. 58, no. 12, pp. 3829–3838, Dec. 2010.
[11] X. Li and Z. Yang, "Dual-printed-dipoles reader antenna for UHF near-field RFID applications," *IEEE Antennas Wireless Propag. Lett.*, vol. 10, pp. 239–242, 2011.
[12] C. Cho, J. Ryoo, I. Park, and H. Choo, "Design of a novel ultra-high frequency radio-frequency identification reader antenna for near-field communications using oppositely directed currents," *Microw. Antennas Propag.*, vol. 4, no. 10, pp. 1543–1548, Oct. 2010.
[13] R. L. Haupt and D. H. Werner, *Genetic Algorithms in Electromagnetics*. Hoboken, NJ: Wiely, 2007.
[14] FEKO Suite 5.5. EM Software and Systems, Stellenbosch, South Africa, 2009 [Online]. Available: http://www.feko.info
[15] "J41," Impinj, Inc., Seattle, WA, 2010 [Online]. Available: http://www.impinj.com
[16] "Speedway RFID Reader," Impinj, Inc., Seattle, WA, 2010 [Online]. Available: http://www.impinj.com